

Published in final edited form as:

*Biochemistry*. 2011 February 8; 50(5): 875–881. doi:10.1021/bi101717b.

## Dnmt3a-CD is Less Susceptible to Bulky Benzo[*a*]pyrene diol epoxide-derived DNA Lesions than Prokaryotic DNA Methyltransferases

Olga V. Lukashevich<sup>‡,||</sup>, Vladimir B. Baskunov<sup>‡,||</sup>, Maria V. Darii<sup>‡,||</sup>, Alexander Kolbanovskiy<sup>⊥</sup>, Alexander A. Baykov<sup>§</sup>, and Elizaveta S. Gromova<sup>‡,\*</sup>

<sup>‡</sup> Chemistry Department, Moscow State University, Moscow, 119991, Russia

<sup>⊥</sup> Department of Chemistry, New York University, 31 Washington Place, New York, NY 10003-5180, USA

<sup>§</sup> A.N. Belozersky Institute of Physico-Chemical Biology, Moscow State University, Moscow, 119991, Russia

### Abstract

Benzo[*a*]pyrene (B[*a*]P) is a well-characterized environmental polycyclic aromatic hydrocarbon pollutant. In living organisms, B[*a*]P is metabolized to the genotoxic *anti*-benzo[*a*]pyrene diol epoxide that reacts with cellular DNA to form stereoisomeric *anti*-B[*a*]PDE-*N*<sup>2</sup>-dG adducts. In this study, we explored the effects of adduct stereochemistry and position in double-stranded DNA substrates on the functional characteristics of the catalytic domain of murine *de novo* DNA methyltransferase Dnmt3a (Dnmt3a-CD). A number of 18-mer duplexes containing site-specifically incorporated (+)- and (–)-*trans-anti*-B[*a*]PDE-*N*<sup>2</sup>-dG lesions located 3'- and 5'-adjacent to and opposite the target cytosine residue were prepared. The Dnmt3a-CD binds cooperatively to the DNA duplexes with an up to 5-fold greater affinity as compared to the undamaged DNA duplexes. Methylation assays showed a 1.7–6.3 fold decrease of the methylation reaction rates for the damaged duplexes. B[*a*]PDE modifications stimulated a non-productive binding and markedly favoured substrate inhibition of Dnmt3a-CD independently of DNA methylation status. The latter effect was sensitive to the position and stereochemistry of the B[*a*]PDE-*N*<sup>2</sup>-dG adducts. The overall effect of *trans-anti*-B[*a*]PDE-*N*<sup>2</sup>-dG adducts on Dnmt3a-CD was less detrimental than in the case of the prokaryotic methyltransferases we previously investigated.

Benzo[*a*]pyrene (B[*a*]P) is an ubiquitous and harmful pollutant that is abundant in car exhaust and tobacco smoke (1), and is metabolically activated to the biologically active benzo[*a*]pyrene-7,8-diol-9,10-epoxides with predominant formation of benzo[*a*]pyrene-7*R*, 8*S*-dihydrodiol-9*S*,10*R*-epoxide ((+)-*anti*-B[*a*]PDE). In the *anti*-orientation of B[*a*]PDE, the 7-OH and 9,10-epoxide groups are on opposite sites of the planar polycyclic aromatic ring system (2,3). Both the (+)- and (–)-*anti*-enantiomers of B[*a*]PDE bind covalently to the exocyclic amino group of guanine, with *trans* or *cis* opening of the epoxide ring. The most abundant adduct is (+)-*trans-anti*-B[*a*]PDE-*N*<sup>2</sup>-dG, both *in vivo* (4) and *in vitro* (about 90%) (5), with lower amounts of the (+)-*cis*- and (–)-*trans-anti*-B[*a*]PDE-*N*<sup>2</sup>-dG adduct being formed when native DNA is reacted with B[*a*]PDE *in vitro* (5). The B[*a*]PDE-DNA adducts affect the functional properties of a variety of enzymes that include, for example,

\* To whom correspondence should be addressed: Tel: +7 495 939 31 44. Fax: +7 495 939 31 81. gromova@genebee.msu.ru.

|| These authors contributed equally to this work.

bacteriophage T7 RNA polymerase (6), replicative (7) and Y-family DNA polymerases (8), HIV-1 integrase (9), vaccinia DNA topoisomerase and *Escherichia coli* exonuclease III (10), human topoisomerase I (11), and human DNA polymerase gamma (12). Furthermore, B[a]PDE-DNA adducts exert significant effects on DNA methylation. The treatment of mouse BALB/3T3 CL1-13 cells with B[a]P resulted in a 12% decrease in the overall 5-methylcytosine content of cellular DNA (13). Another study showed that B[a]P exposure of breast cancer cells led to dynamic sequence-specific hypo- and hypermethylation events identified in a number of genomic repeats (14). The B[a]PDE-*N*<sup>2</sup>-dG adducts strongly affect DNA methylation catalyzed by the prokaryotic DNA methyltransferases (MTases), M.SssI and M.HhaI (15,16), and fully abolish methylation when located 5'-adjacent to the target cytosine (15). High levels of B[a]PDE-DNA adducts inhibit DNA methylation by the eukaryotic MTase Dnmt1 (17).

The methylation of DNA is an epigenetic modification that plays an important role in the control of gene expression in mammalian cells (18). Alterations of the DNA methylation status may constitute a key mechanism in tumorigenesis, since global genomic hypomethylation as well as gene-specific hypermethylation are observed in nearly all types of tumors (19,20). DNA methylation in mammals is carried out by three active MTases, Dnmt1, Dnmt3a, and Dnmt3b, using S-adenosyl-L-methionine as the methyl group donor. Methylation occurs predominantly at the cytosine residues in CpG sequence contexts, yielding 5-methylcytosines (21). Mammalian MTase Dnmt3a is particularly active during embryogenesis, and is commonly thought to be responsible for *de novo* methylation and establishing methylation patterns (22). Recently, the role of Dnmt3a in maintenance DNA methylation has been proposed (23). It was suggested that the bulk of methylation copying is carried out by the maintenance MTase Dnmt1 when DNA is replicated, while Dnmt3a and Dnmt3b complete the methylation process soon after replication and correct errors that are left behind by Dnmt1. Downregulation of Dnmt3a dramatically inhibits the growth and metastasis of malignant melanoma (24) and the replication of colorectal cancer cells (25). Finally, there are indications that direct Dnmt3a-p53 interactions suppress the p53-mediated transcription of tumor suppressor genes (26).

The main objective of this study was to investigate the effects of B[a]PDE-induced DNA damage on methylation carried out by the catalytic domain of murine Dnmt3a. We have uncovered that the enzyme can cooperatively bind to B[a]PDE-DNA adducts with the formation of non-productive complexes, in particular, at high adduct concentrations (substrate inhibition). However, there is little effect of lesions on the catalytic constant at low adduct concentration. Accordingly, we conclude that the overall effects of *trans-anti*-B[a]PDE-*N*<sup>2</sup>-dG adducts on Dnmt3a-CD activity are less severe than those associated with prokaryotic methyltransferases.

## EXPERIMENTAL PROCEDURES

### Chemicals and Buffers

S-Adenosyl-L-homocysteine was purchased from Sigma (St. Louis, MO). [ $\text{CH}_3$ -<sup>3</sup>H]AdoMet (77 Ci/mmol, 13  $\mu\text{M}$ ) was obtained from Amersham Biosciences (Little Chalfont, U.K.), and ( $\gamma$ -<sup>32</sup>P)-ATP (1 Ci/ $\mu\text{mol}$ ) from <<Isotop>> (Obninsk, Russia). B[a]PDE-modified oligodeoxynucleotides (Table 1) were synthesized as described previously (15). Other oligodeoxynucleotides were purchased from Syntol (Moscow, Russia) and IDT (Coralville, IA). The fluorescein label (FAM) was introduced at the 5'-end of the oligodeoxynucleotides using an aminoalkyl linker containing six methylene groups. The oligodeoxynucleotide concentrations were determined spectrophotometrically (27).

The following buffers (B1-B7) were used: B1, 50 mM sodium phosphate (pH 6.0), 1 M NaCl, 10 mM mercaptoethanol, 10% (v/v) glycerol, 0.1% Triton X-100; B2, buffer B1 containing 17 µg/ml phenylmethanesulfonyl chloride, 5 µg/ml leupeptin and 1 µg/ml pepstatin A; B3, B4, and B5, buffer B2 containing 10 mM, 20 mM and 150 mM imidazole-HCl, respectively; B6, 20 mM Tris-HCl (pH 7.4), 0.2 mM EDTA, 2 mM dithiothreitol, 5% (v/v) glycerol; B7, 20 mM HEPES-NaOH (pH 7.0), 100 mM KCl, 1 mM EDTA, 0.2 mM dithiothreitol.

### Enzyme Expression and Purification

The N-terminal His<sub>6</sub> tag fusion catalytic domain of Dnmt3a was expressed in *E. coli* BL21 (DE3) cells (Novagen) using the pET28a plasmid containing Dnmt3a-CD as a vector, as described previously (28). Cells were grown in LB medium at 32°C with intensive aeration until  $A_{600} \sim 0.7$  was attained. Protein expression was initiated by the addition of 1 mM isopropyl β-D-thiogalactopyranoside. After 3 h, cells were harvested by centrifugation at 3000 g for 15 min and disrupted with an MSE Sonifier (Crawley, U.K.) in buffer B2. The cell debris was removed by centrifugation. The supernatant was applied to a Ni-NTA agarose column (BD Biosciences Clontech) equilibrated with B1. After washing with buffers B2, B3 and B4, Dnmt3a-CD was eluted with buffer B5. The eluate was dialyzed overnight against buffer B6, glycerol was added to 50% (v/v), and BSA to a concentration of 200 µg/ml. All protein expression and purification steps were performed at 4°C. The final preparation of Dnmt3a-CD was >90% pure, as assessed with 12.5% Laemmli polyacrylamide gel electrophoresis. The Dnmt3a-CD concentration was determined by the Bradford assay, and expressed in terms of monomer residues.

### Fluorescence Polarization Measurements

Fluorescence polarization was measured using FAM-labeled oligodeoxynucleotide duplexes at 25°C in 500 µL of buffer B7 employing a Beacon 2000 Fluorescence Polarization System (PanVera, USA), with excitation at 488 nm and emission at 535 nm. Oligodeoxynucleotide duplexes (5 nM) containing the FAM label at the 5'-end of one DNA strand (5'-FAM-TCAGAGTGCCTGGCTC or 5'-FAM-TCAGAGTGMGCTTGGCTC) were preincubated with 0.1 mM AdoHcy, and the fluorescence polarization of free DNA ( $P_0$ ) was measured. Dnmt3a-CD was added in 1–5 µL aliquots of a 8.5 µM stock solution to a final concentration of 325–480 nM, and the polarization value ( $P$ ) was recorded 2 min after each addition. The titration was continued until the polarization values reached a constant value ( $P_{\max}$ ) corresponding to fully bound duplexes. In all cases, the titration curves were determined in at least two independent trials. The binding data were analyzed in terms of Scheme 1 (29): where  $E_2$  and  $E_4$  represent the homodimeric and homotetrameric Dnmt3a-CD molecules, respectively, and  $S$  denotes FAM-labeled DNA. The dissociation constants,  $K_{d1}$  and  $K_{d2}$ , were derived from the binding curves by simultaneous fitting equations 1-5 with SCIENTIST from MacroMath (St. Louis, MO) to the fluorescence polarization values  $P$  at different total enzyme concentrations  $[E_2]_0$ :

$$P = P_0 + (P_{\max} - P_0) (0.5 [E_2S] + [E_4S]) / [S]_0 \quad (1)$$

$$[E_2] [S] / [E_2S] = K_{d1} \quad (2)$$

$$[E_2] [E_2S] / [E_4S] = K_{d2} \quad (3)$$

$$[E_2] + [E_2S] + 2[E_4S] = [E_2]_0 \quad (4)$$

$$[S] + [E_2S] + [E_4S] = [S]_0 \quad (5)$$

$[E_2]$  and  $[S]$  represent the free enzyme and substrate concentrations, respectively, while  $[S]_0$  is a total FAM-DNA concentration. The fitting procedure took into account the mass balance and the decrease in concentrations of both free enzyme and DNA upon complex formation.

### Methylation Assays

DNA methylation by Dnmt3a-CD was monitored by measuring the amount of tritium incorporated into the oligodeoxynucleotide duplexes in buffer B7 at 37°C (30). The reaction mixtures contained either 0.1–0.3 μM oligodeoxynucleotide duplex, 1.7–7.6 μM Dnmt3a-CD, and 1.2 μM  $[CH_3-^3H]AdoMet$  (i.e., the enzyme was in an at least 10-fold excess over substrate), or, 2–2.5 μM oligodeoxynucleotide duplex, 0.69 μM Dnmt3a-CD and 2 μM  $[CH_3-^3H]AdoMet$ , representing a 2.9–3.6-fold molar excess of a substrate over the enzyme. The reaction was initiated by the addition of  $[CH_3-^3H]AdoMet$ . After 4–90 min of incubation, 4.9 μl aliquots of the reaction mixtures were pipetted onto DE-81 paper disks (Whatman, Brentford, U.K.). The filters were washed four times with 50 mM  $KH_2PO_4$  and once with water, dried and placed into 5 ml of Zhs-106 scintillation fluid (Reakhim, Russia). The filter-bound radioactivity was measured using a Tracor Analytic Delta 300 scintillation counter (ThermoQuest/CE Instruments, Piscataway, USA), and the amount of methylated DNA was determined according to a previously described protocol (30). The time-course of each of the methylation reactions were fit to Eq 6, where  $[P]$  and  $[P]_{lim}$  represent the concentrations of methylated DNA at time  $t$ , and infinity, respectively, and  $k$  is the apparent rate constant of methylation:

$$[P] = [P]_{lim} (1 - e^{-kt}) \quad (6)$$

The initial rate of the methylation reaction ( $v$ ) was calculated from the relationship  $v = k[P]_{lim}$ , and the final yield of the methylated product ( $R$ ) was calculated as  $[P]_{lim}/[S]_0$ , where  $[S]_0$  represents the initial substrate concentration. In experiments measuring only the initial linear parts of the product formation curves, the initial rates of methylation were directly determined from the slopes of these curves, as eq 6 can be approximated by  $[P] = kt[P]_{lim}$  in this case.

## RESULTS

The aim of the present study was to determine whether (+)- and (–)-*trans-anti*-B[a]PDE- $N^2$ -dG lesions (hereafter designated  $B^+$  and  $B^-$ , respectively) (Fig. 1) affect the function of Dnmt3a-CD. We employed the catalytic domain of Dnmt3a, which has a catalytic activity similar to that of the wild-type enzyme (31,32). Ten different 18-mer oligodeoxynucleotide duplexes with  $B^+$  or  $B^-$  incorporated in one strand of the unmethylated or hemimethylated DNA duplexes within or adjacent to the 5'-side of the Dnmt3a-CD recognition sequence, were prepared (Table 1). Three families of B[a]PDE-damaged duplexes derived from 18-mer undamaged control duplexes GCGC/CGCG, GCGC/CGMG, and GMGC/CGCG were employed in our studies (Table 2). Hemimethylated substrates contained  $m^5dC$  instead of target dC either in the strand with damaged guanine (GMGC/CGCG family) or in the

complementary strand (GCGC/CGMG family). The methylation rates and catalytic constants obtained under conditions of enzyme or DNA excess, as well as the dissociation constants for these three families of DNA duplexes are summarized in Table 2.

### Effects of B[a]PDE-derived lesions on Dnmt3a-CD Binding

Typical binding curves obtained upon titration of the FAM-labeled 18-mer DNA duplexes with Dnmt3a-CD using a fluorescence polarization technique are presented in Fig. 2. The binding curves of duplexes not shown in this Figure exhibited similar behavior. The co-factor analog, AdoHcy, was added to mimic the experimental conditions of the methylation assays. The binding curves are clearly sigmoidal in shape for the damaged as well as the undamaged DNA duplexes. These results are consistent with the earlier findings that the interactions of Dnmt3a-CD with undamaged and 8-oxoG-containing 30-mer DNA duplexes are characterized by a positively cooperative mode of binding (29).

The curves can be interpreted in terms of Scheme 1, yielding two macroscopic binding constants,  $K_{d1}$  and  $K_{d2}$  (Table 2), for binding of the two Dnmt3a-CD homodimers to the DNA duplex. As shown in Table 2,  $K_{d1}$  exceeded  $K_{d2}$  in all cases, whereas  $K_{d1}/K_{d2} = 0.25$  is expected for non-cooperative binding (33). The difference between  $K_{d1}$  and  $K_{d2}$  was particularly large in the case of the duplex GCGC/CGMG and its B[a]PDE-derivatives, thus making the fraction of the  $E_2S$  complex insignificant over the whole range of enzyme concentrations and preventing an evaluation of the magnitudes of the individual binding constants. For these duplexes, only the product  $K_{d1}K_{d2}$  could be estimated for comparison with other duplexes.

The binding affinities for B[a]PDE-damaged duplexes, characterized by the values of the dissociation constants product  $K_{d1}K_{d2}$ , were higher than for the corresponding undamaged duplexes in all families (Table 2), except for GCB<sup>+</sup>C/CGCG. Notably, the  $K_{d1}$  values were more sensitive to the B[a]PDE-DNA adducts than the  $K_{d2}$  values. This finding is consistent with the mode of binding of Dnmt3a, when the second Dnmt3a dimer is attracted to the DNA molecule by interactions with the first, already bound Dnmt3a dimer, a mechanism that should be less sensitive to the presence of the B[a]PDE residues.

### Effects of B[a]PDE-derived Lesions on Dnmt3a-CD Catalysis

The rates of methylation  $v_1$  and  $v_2$  were measured at two different sets of enzyme and DNA concentrations: enzyme in excess over substrate or substrate in excess over enzyme (Table 2). In the first case, the measurements spanned the complete time course of the reactions (Fig. 3), and the time course of the reaction was well described by an exponential function (Eq. 6). As the substrate conversion was relatively low in the second set of measurements, the product formation curves were linear (Fig. 4), allowing for the direct determination of the initial rates of methylation ( $v_2$ ) from the slopes. The amounts of methylated products accumulating at the end of the incubation period did not exceed the enzyme concentration in either case, which is indicative of single-turnover conditions. It is worth noting that introduction of B[a]PDE residue into DNA had virtually no effect on  $v_1$  values, which were changed by only 1.4-2-fold compared to those for the corresponding undamaged substrates. In contrast, the  $v_2$  values were in most cases decreased by the B[a]PDE modifications, by a factor of 1.7–6.3.

The initial rates estimated in the two types of assays ( $v_1$  and  $v_2$  in Table 2) are not directly comparable because the experiments were conducted at different enzyme-substrate concentrations. Therefore,  $v_1$  and  $v_2$  were converted to apparent catalytic rate constants ( $k_{cat,1}$  and  $k_{cat,2}$ , respectively) by dividing these values by the corresponding initial  $E_4S$  concentrations. The latter was calculated in each case from the total enzyme and substrate

concentrations using the  $K_{d1}$  and  $K_{d2}$  values determined from the fluorescence titration experiments (Table 2), which was justified by the fact that the FAM label does not affect the DNA-MTase interactions (27). In experiments measuring  $v_1$ , nearly all of added substrate was present in the form of the  $E_4S$  complex, whereas 32–88% of the added enzyme formed  $E_4S$  complexes in the experiments designed to determine  $v_2$ . The  $k_{cat,1}$  and  $k_{cat,2}$  estimations were based on the earlier finding that  $E_4S$  is the only catalytically competent complex in this system. The  $E_4S$  stoichiometry of the substrate complex is consistent with the crystal structure of Dnmt3a-CD complexed with its orthologous protein Dnmt3L, gel-filtration data and the results of mutational analysis (32,34). Furthermore, this stoichiometry is supported by comparison of  $P_{max} - P_0$  values for the complexes of GCGC/CGCG with Dnmt3a-CD (0.25–0.26) and M.SssI (0.08–0.09) (data not shown), if one takes into account that the subunit masses of these enzymes are 36 and 44 kDa, respectively, and that M.SssI binds as monomer. Similar stoichiometries were reported for complexes with 30-mer duplexes (29).

The  $k_{cat,1}$  values, derived from enzymatic activities measured at low free substrate concentrations, were several fold lower for the hemimethylated DNA duplexes derived from GMGC/CGCG and GCGC/CGMG than for unmethylated duplexes derived from GCGC/CGCG, but were not significantly affected by the B[a]PDE- $N^2$ -dG-adducts (Table 2). In contrast, the  $k_{cat,2}$  values obtained from the activities measured at high free substrate concentrations displayed more marked variations within each of the three different families of DNA duplexes. In general, B[a]PDE- $N^2$ -dG lesions led to a decrease in  $k_{cat,2}$  by a factor of 2–7. Furthermore, in most cases, the  $k_{cat,2}$  values were lower than the  $k_{cat,1}$  values, indicative of substrate inhibition, apparently resulting from non-productive binding of additional substrate molecule(s) at high substrate concentration (33,35,36). A difference in the catalytic constants for the damaged substrates varied in the three families of duplexes. The largest difference between  $k_{cat,1}$  and  $k_{cat,2}$  (up to 12-fold) values was observed with B[a]PDE-damaged unmethylated substrates, but no inhibition was evident with one such substrate (B<sup>+</sup>CGC/CGCG). Undamaged substrates showed little substrate inhibition, both in the unmethylated and hemimethylated forms.

Notably, substrate inhibition was negligible at free substrate concentration below 10 nM that were used in the  $k_{cat,1}$  measurements. Therefore, the  $k_{cat,1}$  values refer to the true catalytic constant of Dnmt3a-CD. The differences in  $k_{cat,2}$  values mainly reflect the effects of the structure of the substrate on its ability to form non-productive complex with Dnmt3a-CD at the higher DNA substrate concentrations.

### Formation of non-productive complexes

The final yields ( $R$ ) of methylated products were estimated in assays performed under conditions of enzyme excess. In the case of hemimethylated duplexes, the concentrations of methylated DNA at the end of the reaction were lower than the initial substrate concentrations (0.3  $\mu$ M) in all cases (Fig. 3). Based on results of experiments with other substrate analogs (29), these phenomenon can be explained in terms of the formation of non-productive enzyme-substrate complexes. The reaction virtually stops after all of the productive complexes are converted, leaving the substrate intact in the non-productive complexes, which dissociates very slowly. The  $R$  value may thus vary from 100% (non-productive binding does not occur) to 0% (all of the complexes are non-productive).

For the undamaged, unmethylated substrate (GCGC/CGCG), the  $R$  value was nearly 100%, but decreased significantly in the case of the hemimethylated DNA duplexes (GMGC/CGCG and GCGC/CGMG) (Table 2 and Fig. 3A), indicating considerable non-productive substrate binding. The introduction of B[a]PDE- $N^2$ -dG-adducts further decreased the  $R$  value by approximately 1.5–2-fold (Table 2 and Fig. 3B), the effect being somewhat larger

in the case of hemimethylated duplexes in which damaged dG was located in the unmethylated strand.

## DISCUSSION

### Interactions of Dnmt3a-CD with Non-damaged Substrates

As shown previously, two dimeric Dnmt3a-CD molecules bind cooperatively to 30-mer DNA duplexes to form a catalytically competent  $E_4S$  complex (29). The present results suggest that the 18-mer DNA duplexes behave similarly to 30-mer duplexes. Specifically, the sigmoidicity of the binding curves in Fig. 2 indicates that two dimeric Dnmt3a-CD molecules bind per DNA duplex and the binding curves exhibit positive cooperativity. The binding affinity is slightly lower, i.e., the  $K_{d1}K_{d2}$  value is  $4400 \text{ nM}^2$  for the 18-mer GCGC/CGMG duplex (Table 2) versus  $830 \text{ nM}^2$  for a 30-mer GCGC/CGMG duplex (29). This difference is entirely attributable to the  $K_{d1}$  value since  $K_{d2}$  values are similar for both duplexes (Table 2 and (29)).

Based on the  $R$  values, some inferences can be made on the mode of Dnmt3a-CD binding to DNA. The yields of the methylated products ( $R$ ) obtained with GCGC/CGCG, GMGC/CGCG and GCGC/CGMG duplexes as substrates were 95:64:28 (Table 2). The  $R$  values less than 100% for the hemimethylated duplexes suggest that the active site is oriented towards the already methylated cytosine in the non-productive complex of Dnmt3a-CD. This hypothesis is in agreement with the previous data showing both productive and non-productive binding of 30-mer hemimethylated duplexes (29). The ability of Dnmt3a-CD to bind to methylated strand stems from the observation that the enzyme can interact with fully methylated DNA (29). That the  $R$  values are higher for the GMGC/CGCG duplex than for the GCGC/CGMG duplex may indicate preferential Dnmt3a-CD binding to DNA from the side of the bottom strand (TCAGAGTGCCTTGGCTC and TCAGAGTGMGCTTGGCTC, respectively) in both duplexes, consistent with the preferential methylation of  $\text{Py}^{-2}\text{Pu}^{-1}\text{CGPy}^{+1}$  sequence by Dnmt3a (Py and Pu represent pyrimidine and purine nucleotide, respectively) (37,38). Based on this, one can further speculate that flanking sequence has a stronger effect on Dnmt3a-CD binding to DNA than the methylation status of the target cytosine.

Interestingly, both  $k_{\text{cat},1}$  and  $R$  values for the duplex GMGC/CGCG ( $2.5 \text{ h}^{-1}$  and 64%, respectively) are higher than those for the duplex GCGC/CGMG ( $1.4 \text{ h}^{-1}$  and 28%, respectively). This correlation between the  $k_{\text{cat},1}$  and  $R$  values may mean that the decreased  $k_{\text{cat},1}$  value for the latter duplex results solely from increased non-productive binding. However, more extensive data are needed to further test this hypothesis.

### Interactions of Dnmt3a-CD with B[a]PDE-damaged DNA

The introduction of one  $B^+$  or  $B^-$  lesion stimulated the binding of 18-mer DNA duplexes to Dnmt3a-CD (Table 2), as characterized by the  $K_{d1}$  and  $K_{d2}$  values. The accompanying decrease in  $R$  suggests that this effect results, at least partly, from the formation of non-productive binding. The increased stabilities of the complexes may result from the contribution of hydrophobic interactions between the B[a]PDE residues and the enzyme. The benzo[a]pyrenyl moieties are positioned in the minor groove of DNA, oriented either towards the 5'- or the 3'-end of the modified strand in the case of the stereoisomeric adducts in the  $B^+$  and  $B^-$  duplexes, respectively (39,40). However, the catalytic constant estimated at low substrate concentrations ( $k_{\text{cat},1}$ ) was only slightly affected by the B[a]PDE- $N^2$ -dG adducts.

The major effect of the B[a]PDE- $N^2$ -dG lesions is to suppress Dnmt3a-CD activity at high substrate concentrations ( $k_{\text{cat},2}$ ), i.e., to induce strong substrate inhibition. Purdy and co-

workers (41) recently reported that there was no inhibition of Dnmt3a-CD activity by unmodified DNA substrates. Our data consistently show that substrate inhibition of Dnmt3a-CD by undamaged 18-mer unmethylated and hemimethylated DNA duplexes is quite small (within the experimental error of  $k_{cat,1}$  and  $k_{cat,2}$ ) (Table 2). In contrast, DNA duplexes containing the B[a]PDE- $N^2$ -dG adducts, except B<sup>+</sup>CGC/CGCG and, possibly, B<sup>+</sup>CGC/CGMG, demonstrate strong substrate inhibition of Dnmt3a-CD ( $k_{cat,1}/k_{cat,2} \sim 4-12$ ). In order for  $k_{cat}$  to drop by a factor of 4-12 at the free substrate concentration of approximately 2  $\mu$ M, as used in  $k_{cat,2}$  measurements, the binding constant describing binding of the inhibiting substrate molecule(s) should be well below 1  $\mu$ M. The inhibiting substrate molecule(s) may either decrease the true catalytic constant of the productive complex or further decrease  $R$  value (i.e., further stimulate non-productive binding). Notably, the  $R$  values in Table 2 were derived from assays performed in the absence of substrate inhibition, and may not be the same as those of the substrate-inhibited complexes. We cannot distinguish between these alternatives at present because both effects are expected to decrease the observed  $k_{cat}$  value. Another corollary is that Scheme 1 is valid only at low substrate concentrations, such as those employed in fluorescence titration experiments and  $v_1$  measurements, and should be supplemented with an  $E_4S_2$  complex at high substrate concentrations.

The stereochemistry of the B[a]PDE- $N^2$ -dG adduct does not appear to be important when located within the CpG site, since the  $R$ ,  $k_{cat,1}$  and  $k_{cat,2}$  values are similar for the (+)- and (-)-adduct forms (Table 2). However, the stereochemistry is clearly important when the adduct is located on the 5'-side and adjacent to the target cytosine.

Recent studies have shown that the B[a]PDE- $N^2$ -dG-adducts strongly affect DNA methylation catalyzed by the prokaryotic MTases, M.EcoRII, M.HhaI, and M.SssI (15,27). In fact, methylation by M.HhaI and M.SssI was completely abolished when B<sup>+</sup> or B<sup>-</sup> was located on the 5'-side and adjacent to the target cytosine (15). Dnmt3a-CD is therefore considerably less sensitive to these adducts since it displays significant methylation activity although at a several-fold smaller rate. Moreover, the B[a]PDE residues decrease the DNA affinity of M.HhaI up to 100-fold, whereas the same DNA lesions enhance the binding of Dnmt3a-CD to the DNA 4-5 fold. Therefore, we conclude that the methylation activity of Dnmt3a-CD is less affected by the B[a]PDE- $N^2$ -dG adducts compared with the prokaryotic MTases. While the evolutionary advantage of such "desensitization" is evident, the elucidation of the underlying mechanism should await determination of three-dimensional structures of the complexes of these enzymes with DNA.

The effects of the B[a]PDE-derived lesions on Dnmt3a-CD differ from those of 7,8-dihydro-8-oxoguanine (8-oxoG), another frequently occurring DNA lesion associated with oxidative stress and also with normal cellular metabolism (42). Guanine oxidation to 8-oxoG generates a strong hydrogen bond acceptor at C8 and converts N7 from a proton acceptor to donor, thus altering the hydrogen bond network between the Dnmt3a-CD and the DNA (29). As a result, the binding of hemimethylated DNA duplexes containing 8-oxoG 5'-adjacent to the target cytosine by Dnmt3a-CD is weakened by a factor of 17, and the rate of methylation determined under conditions of DNA excess is decreased by a factor of 4 (29). The minor groove B[a]PDE- $N^2$ -dG adduct produces similar changes in DNA methylation, and the opposite effect on Dnmt3a-CD binding.

In summary, the B[a]PDE-DNA adducts stimulate the binding of Dnmt3a-CD to DNA, enhance the probability of formation of non-productive complexes, and markedly promote substrate inhibition of Dnmt3a-CD. The latter effect is sensitive to the position and the stereochemistry of the adducts. However, the overall effect of B[a]PDE damage on Dnmt3a-CD is less detrimental than it is in the case of prokaryotic methyltransferases.



## Acknowledgments

We thank Prof. A. Jeltsch for the Dnmt3a-CD plasmid. We are grateful to Prof. N.E. Geacintov for critically reading the manuscript and helpful discussion.

This research was supported by RFBR Grants 09-04-00869, 10-04-00809, 08-04-91109/CRDF RUB1-2919-MO-07, and NIH/NCI grant CA099194.

## Abbreviations

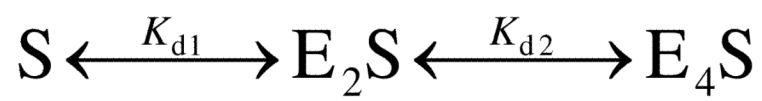
<b>AdoHcy</b>	S-adenosyl-L-homocysteine
<b>AdoMet</b>	S-adenosyl-L-methionine
<b>B[a]P</b>	benzo[a]pyrene
<b>anti-B[a]PDE</b>	<i>r</i> 7, <i>t</i> 8-dihydroxy- <i>t</i> 9,10-epoxy-7,8,9,10-tetrahydrobenzo[a]pyrene
<b>B<sup>+</sup> and B<sup>-</sup></b>	(+)- or (-)- <i>trans-anti</i> -B[a]PDE- <i>N</i> <sup>2</sup> -dG, respectively
<b>Dnmt3a</b>	DNA methyltransferase Dnmt3a
<b>Dnmt3a-CD</b>	catalytic domain of Dnmt3a
<b>EDTA</b>	disodium ethylenediaminetetraacetate
<b>FAM</b>	6(5)-carboxyfluorescein
<b>M</b>	5-methylcytosine
<b>MTase</b>	DNA-(cytosine C5)-methyltransferase

## REFERENCES

1. Phillips DH. Fifty years of benzo(a)pyrene. *Nature*. 1983; 303:468–472. [PubMed: 6304528]
2. Conney AH, Chang RL, Jerina DM, Wei SJ. Studies on the metabolism of benzo[a]pyrene and dose-dependent differences in the mutagenic profile of its ultimate carcinogenic metabolite. *Drug Metab Rev*. 1994; 26:125–163. [PubMed: 8082562]
3. Boysen G, Hecht SS. Analysis of DNA and protein adducts of benzo[a]pyrene in human tissues using structure-specific methods. *Mutat Res*. 2003; 543:17–30. [PubMed: 12510015]
4. Weinstein IB, Jeffrey AM, Jennette KW, Blobstein SH, Harvey RG, Harris C, Autrup H, Kasai H, Nakanishi K. Benzo(a)pyrene diol epoxides as intermediates in nucleic acid binding in vitro and in vivo. *Science*. 1976; 193:592–595. [PubMed: 959820]
5. Cheng SC, Hilton BD, Roman JM, Dipple A. DNA adducts from carcinogenic and noncarcinogenic enantiomers of benzo[a]pyrene dihydrodiol epoxide. *Chem Res Toxicol*. 1989; 2:334–340. [PubMed: 2519824]
6. Choi DJ, Marino-Alessandri DJ, Geacintov NE, Scicchitano DA. Site-specific benzo[a]pyrene diol epoxide-DNA adducts inhibit transcription elongation by bacteriophage T7 RNA polymerase. *Biochemistry*. 1994; 33:780–787. [PubMed: 8292606]
7. Shibutani S, Margulis LA, Geacintov NE, Grollman AP. Translesional synthesis on a DNA template containing a single stereoisomer of dG-(+)- or dG-(-)-anti-BPDE (7,8-dihydroxy-anti-9,10-epoxy-7,8,9,10-tetrahydrobenzo[a]pyrene). *Biochemistry*. 1993; 32:7531–7541. [PubMed: 8338850]
8. Rechkoblit O, Zhang Y, Guo D, Wang Z, Amin S, Krzeminsky J, Louneva N, Geacintov NE. *trans*-Lesion synthesis past bulky benzo[a]pyrene diol epoxide N2-dG and N6-dA lesions catalyzed by DNA bypass polymerases. *J Biol Chem*. 2002; 277:30488–30494. [PubMed: 12063247]
9. Johnson AA, Sayer JM, Yagi H, Patil SS, Debart F, Maier MA, Corey DR, Vasseur JJ, Burke TR Jr, Marquez VE, Jerina DM, Pommier Y. Effect of DNA modifications on DNA processing by HIV-1 integrase and inhibitor binding: role of DNA backbone flexibility and an open catalytic site. *J Biol Chem*. 2006; 281:32428–32438. [PubMed: 16943199]

10. Yakovleva L, Handy CJ, Yagi H, Sayer JM, Jerina DM, Shuman S. Intercalating polycyclic aromatic hydrocarbon-DNA adducts poison DNA religation by Vaccinia topoisomerase and act as roadblocks to digestion by exonuclease III. *Biochemistry*. 2006; 45:7644–7653. [PubMed: 16768460]
11. Pommier Y, Kohlhagen G, Laco GS, Kroth H, Sayer JM, Jerina DM. Different effects on human topoisomerase I by minor groove and intercalated deoxyguanosine adducts derived from two polycyclic aromatic hydrocarbon diol epoxides at or near a normal cleavage site. *J Biol Chem*. 2002; 277:13666–13672. [PubMed: 11832494]
12. Graziewicz MA, Sayer JM, Jerina DM, Copeland WC. Nucleotide incorporation by human DNA polymerase gamma opposite benzo[a]pyrene and benzo[c]phenanthrene diol epoxide adducts of deoxyguanosine and deoxyadenosine. *Nucleic Acids Res*. 2004; 32:397–405. [PubMed: 14729924]
13. Wilson VL, Jones PA. Inhibition of DNA methylation by chemical carcinogens in vitro. *Cell*. 1983; 32:239–246. [PubMed: 6825170]
14. Sadikovic B, Andrews J, Rodenhiser DI. DNA methylation analysis using CpG microarrays is impaired in benzo[a]pyrene exposed cells. *Toxicol Appl Pharmacol*. 2007; 225:300–309. [PubMed: 17904174]
15. Subach OM, Baskunov VB, Darii MV, Maltseva DV, Alexandrov DA, Kirsanova OV, Kolbanovskiy A, Kolbanovskiy M, Johnson F, Bonala R, Geacintov NE, Gromova ES. Impact of benzo[a]pyrene-2'-deoxyguanosine lesions on methylation of DNA by SssI and HhaI DNA methyltransferases. *Biochemistry*. 2006; 45:6142–6159. [PubMed: 16681387]
16. Subach OM, Maltseva DV, Shastri A, Kolbanovskiy A, Klimasauskas S, Geacintov NE, Gromova ES. The stereochemistry of benzo[a]pyrene-2'-deoxyguanosine adducts affects DNA methylation by SssI and HhaI DNA methyltransferases. *FEBS J*. 2007; 274:2121–2134. [PubMed: 17388812]
17. Ruchirawat M, Becker FF, Lapeyre JN. Mechanism of rat liver DNA methyltransferase interaction with anti-benzo[a]pyrenediol epoxide modified DNA templates. *Biochemistry*. 1984; 23:5426–5432. [PubMed: 6095897]
18. Turek-Plewa J, Jagodzinski PP. The role of mammalian DNA methyltransferases in the regulation of gene expression. *Cell Mol Biol Lett*. 2005; 10:631–647. [PubMed: 16341272]
19. Ehrlich M. DNA methylation in cancer: too much, but also too little. *Oncogene*. 2002; 21:5400–5413. [PubMed: 12154403]
20. Kanai Y. Alterations of DNA methylation and clinicopathological diversity of human cancers. *Pathol Int*. 2008; 58:544–558. [PubMed: 18801069]
21. Jeltsch A. Beyond Watson and Crick: DNA methylation and molecular enzymology of DNA methyltransferases. *Chembiochem*. 2002; 3:274–293. [PubMed: 11933228]
22. Okano M, Bell DW, Haber DA, Li E. DNA methyltransferases Dnmt3a and Dnmt3b are essential for de novo methylation and mammalian development. *Cell*. 1999; 99:247–257. [PubMed: 10555141]
23. Jones PA, Liang G. Rethinking how DNA methylation patterns are maintained. *Nat Rev Genet*. 2009; 10:805–811. [PubMed: 19789556]
24. Deng T, Kuang Y, Wang L, Li J, Wang Z, Fei J. An essential role for DNA methyltransferase 3a in melanoma tumorigenesis. *Biochem Biophys Res Commun*. 2009; 387:611–616. [PubMed: 19632198]
25. Ng EK, Tsang WP, Ng SS, Jin HC, Yu J, Li JJ, Rocken C, Ebert MP, Kwok TT, Sung JJ. MicroRNA-143 targets DNA methyltransferases 3A in colorectal cancer. *Br J Cancer*. 2009; 101:699–706. [PubMed: 19638978]
26. Wang YA, Kamarova Y, Shen KC, Jiang Z, Hahn MJ, Wang Y, Brooks SC. DNA methyltransferase-3a interacts with p53 and represses p53-mediated gene expression. *Cancer Biol Ther*. 2005; 4:1138–1143. [PubMed: 16131836]
27. Baskunov VB, Subach FV, Kolbanovskiy A, Kolbanovskiy M, Eremin SA, Johnson F, Bonala R, Geacintov NE, Gromova ES. Effects of benzo[a]pyrenedeoxyguanosine lesions on DNA methylation catalyzed by EcoRII DNA methyltransferase and on DNA cleavage effected by EcoRII restriction endonuclease. *Biochemistry*. 2005; 44:1054–1066. [PubMed: 15654762]

28. Gowher H, Jeltsch A. Enzymatic properties of recombinant Dnmt3a DNA methyltransferase from mouse: the enzyme modifies DNA in a non-processive manner and also methylates non-CpG [correction of non-CpA] sites. *J Mol Biol.* 2001; 309:1201–1208. [PubMed: 11399089]
29. Maltseva DV, Baykov AA, Jeltsch A, Gromova ES. Impact of 7,8-dihydro-8-oxoguanine on methylation of the CpG site by Dnmt3a. *Biochemistry.* 2009; 48:1361–1368. [PubMed: 19161295]
30. Brennan CA, Van Cleve MD, Gumpert RI. The effects of base analogue substitutions on the methylation by the EcoRI modification methylase of octadeoxyribonucleotides containing modified EcoRI recognition sequences. *J Biol Chem.* 1986; 261:7279–7286. [PubMed: 3011781]
31. Gowher H, Jeltsch A. Molecular enzymology of the catalytic domains of the Dnmt3a and Dnmt3b DNA methyltransferases. *J Biol Chem.* 2002; 277:20409–20414. [PubMed: 11919202]
32. Jia D, Jurkowska RZ, Zhang X, Jeltsch A, Cheng X. Structure of Dnmt3a bound to Dnmt3L suggests a model for de novo DNA methylation. *Nature.* 2007; 449:248–251. [PubMed: 17713477]
33. Dixon, M.; Webb, EC.; Thorne, CJR.; Tipton, KF. *Enzymes*. 3rd ed.. Longman Group Ltd.; London: 1979. p. 140-148.
34. Jurkowska RZ, Anspach N, Urbanke C, Jia D, Reinhardt R, Nellen W, Cheng X, Jeltsch A. Formation of nucleoprotein filaments by mammalian DNA methyltransferase Dnmt3a in complex with regulator Dnmt3L. *Nucleic Acids Res.* 2008; 36:6656–6663. [PubMed: 18945701]
35. Segel, IH. *Enzyme Kinetics: Behavior and Analysis of Rapid Equilibrium and Steady-State Enzyme Systems*. John Wiley & Sons; New York: 1993.
36. Cornish-Bowden, A. *Fundamentals of Enzyme Kinetics*. Portland Press; London: 1995.
37. Lin IG, Han L, Taghva A, O'Brien LE, Hsieh CL. Murine de novo methyltransferase Dnmt3a demonstrates strand asymmetry and site preference in the methylation of DNA in vitro. *Mol Cell Biol.* 2002; 22:704–723. [PubMed: 11784849]
38. Handa V, Jeltsch A. Profound flanking sequence preference of Dnmt3a and Dnmt3b mammalian DNA methyltransferases shape the human epigenome. *J Mol Biol.* 2005; 348:1103–1112. [PubMed: 15854647]
39. Cosman M, de los Santos C, Fiala R, Hingerty BE, Singh SB, Ibanez V, Margulis LA, Live D, Geacintov NE, Broyde S, et al. Solution conformation of the major adduct between the carcinogen (+)-anti-benzo[a]pyrene diol epoxide and DNA. *Proc Natl Acad Sci U S A.* 1992; 89:1914–1918. [PubMed: 1311854]
40. de los Santos C, Cosman M, Hingerty BE, Ibanez V, Margulis LA, Geacintov NE, Broyde S, Patel DJ. Influence of benzo[a]pyrene diol epoxide chirality on solution conformations of DNA covalent adducts: the (–)-trans-anti-[BP]G.C adduct structure and comparison with the (+)-trans-anti-[BP]G.C enantiomer. *Biochemistry.* 1992; 31:5245–5252. [PubMed: 1606148]
41. Purdy MM, Holz-Schietinger C, Reich NO. Identification of a second DNA binding site in human DNA methyltransferase 3A by substrate inhibition and domain deletion. *Arch Biochem Biophys.* 2010; 498:13–22. [PubMed: 20227382]
42. Valko M, Rhodes CJ, Moncol J, Izakovic M, Mazur M. Free radicals, metals and antioxidants in oxidative stress-induced cancer. *Chem Biol Interact.* 2006; 160:1–40. [PubMed: 16430879]

**Scheme 1.**

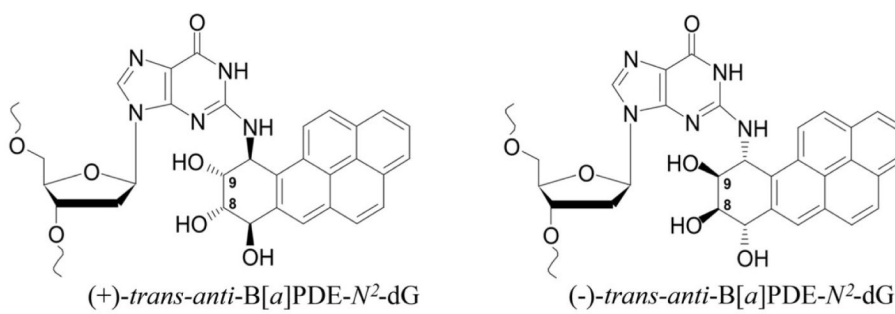


**Fig. 1.**  
Structure of (+) and (-)-*trans-anti*-B[a]PDE-*N*<sup>2</sup>-dG adducts.

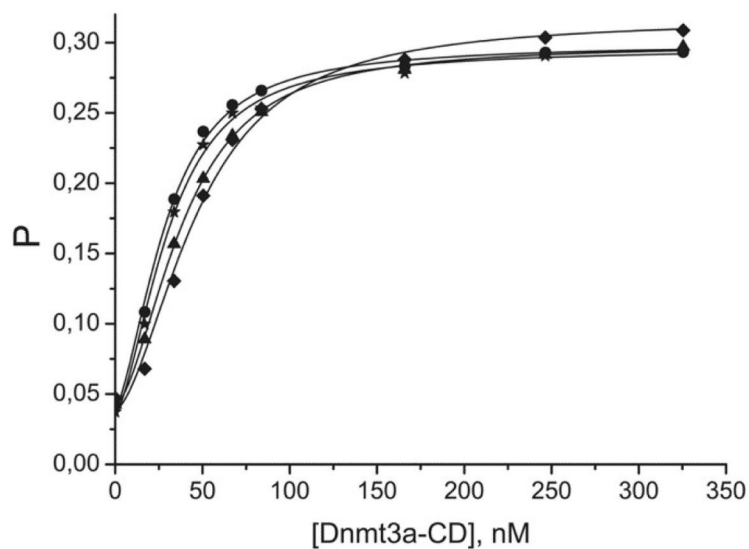


**Fig. 2.** Binding curves obtained upon titration of B[a]PDE-damaged fluorescein-labeled DNA duplexes (10 nM) with increasing amounts of Dnmt3a-CD in the presence of AdoHcy (0.1 mM). P represents the fluorescence polarization value. Total monomeric enzyme concentration is presented. Designations are: (●) B<sup>-</sup>CGC/CGMG, (▲) B<sup>+</sup>CGC/CGMG, (☆) GCB<sup>-</sup>C/CGMG, (◆) GCB<sup>+</sup>C/CGMG.

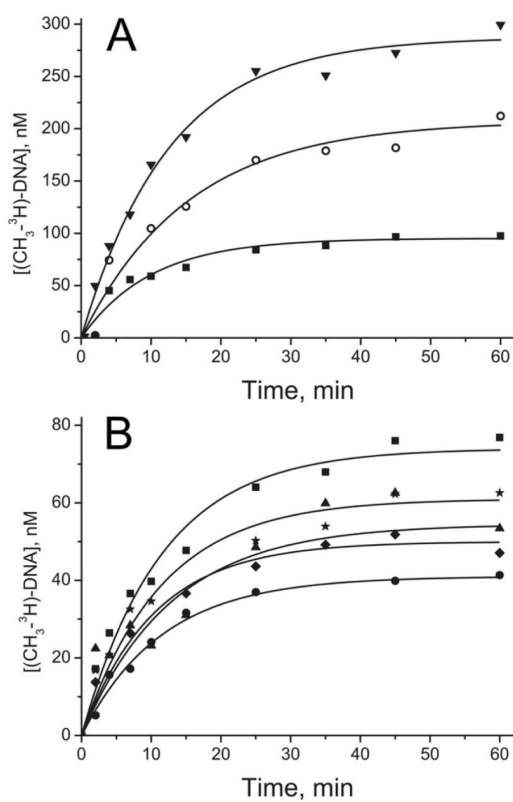


**Fig. 3.** Time-courses of methylation of selected B[a]PDE-damaged (A) and non-damaged (B) DNA duplexes by Dnmt3a-CD under conditions of enzyme excess over DNA. The reaction mixtures contained 300 nM DNA, 5.2-7.6  $\mu\text{M}$  Dnmt3a-CD and 2  $\mu\text{M}$   $[\text{CH}_3\text{-}^3\text{H}]\text{AdoMet}$ . Designations in (A) are: (▼) GCGC/CGCG, (○) GMGC/CGCG, (■) GCGC/CGMG, while those in (B) are as specified for Fig. 2.

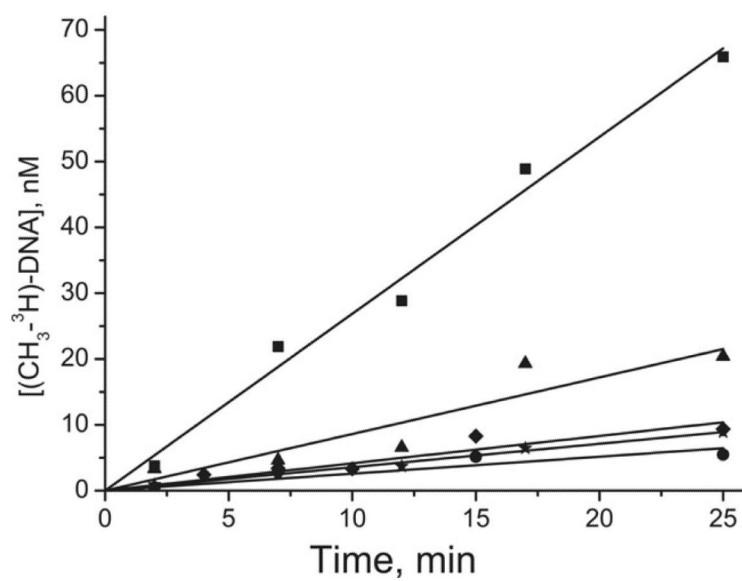


**Fig. 4.** Time-courses of methylation of selected B[a]PDE-damaged duplexes by Dnmt3a-CD under conditions of DNA excess over enzyme. The reaction mixtures contained 2–2.5  $\mu\text{M}$  DNA, 0.69  $\mu\text{M}$  Dnmt3a-CD, and 2  $\mu\text{M}$   $[\text{CH}_3\text{-}^3\text{H}]\text{AdoMet}$ . Designations are as specified for Fig. 3B.



**Table 1**Oligodeoxynucleotide sequences<sup>a</sup>

Designation	Sequence
GCGC	5'GAGCCAAGCGCACTCTGA
GMGC	5'GAGCCAAGMGCCTCTGA
B <sup>-</sup> CGC	5'GAGCCAAB <sup>-</sup> CGCACTCTGA
B <sup>+</sup> CGC	5'GAGCCAAB <sup>+</sup> CGCACTCTGA
GCB <sup>-</sup> C	5'GAGCCAAGCB <sup>-</sup> CACTCTGA
GCB <sup>+</sup> C	5'GAGCCAAGCB <sup>+</sup> CACTCTGA
GMB <sup>-</sup> C	5'GAGCCAAGMB <sup>-</sup> CACTCTGA
GMB <sup>+</sup> C	5'GAGCCAAGMB <sup>+</sup> CACTCTGA
CGCG	5'TCAGAGTGCCTTGGCTC
CGMG	5'TCAGAGTGMCTTGGCTC

<sup>a</sup>M, 5-methylcytosine; B<sup>+</sup> or B<sup>-</sup>, (+)- or (-)-*trans-anti*-B[*a*]PDE-*N*<sup>2</sup>-dG, respectively.

**Table 2**  
Binding and kinetic parameters for parental and B[*a*]PDE-damaged DNA duplexes as substrates of Dnm13a-CD

DNA duplex <sup>e</sup>	$K_{d1}$ (nM)	$K_{d2}$ (nM)	$K_{d1}K_{d2}$ (nM <sup>2</sup> )	$R^b$ (%)	$v_1^c$ (nM/min)	$v_2$ (nM/min)	$k_{cat,1}^d$ (h <sup>-1</sup> )	$k_{cat,2}^e$ (h <sup>-1</sup> )
GCGC CGCG	104 ± 26	34 ± 10	3540	95 ± 4	25 ± 4	3.0 ± 0.3	5.2	2.7
B <sup>-</sup> CGC CGCG	187 ± 54	9 ± 3	1680	94 ± 4	34 ± 6	1.16 ± 0.03	6.9	0.59
B <sup>-</sup> CGC CGCG	49 ± 12	26 ± 6	1270	100 ± 3	17 ± 1	3.1 ± 0.3	3.4	3.7
GCB <sup>-</sup> C CGCG	70 ± 25	18 ± 7	1260	70 ± 6	27 ± 6	1.1 ± 0.1	5.5	0.88
GCB <sup>+</sup> C CGCG	190 ± 59	21 ± 7	3930	74 ± 5	30 ± 7	0.85 ± 0.03	6.2	0.54
GMGC CGCG	170 ± 90	22 ± 6	3720	64 ± 4	12 ± 2	2.6 ± 0.2	2.5	1.8
GMB <sup>-</sup> C CGCG	73 ± 23	30 ± 11	2190	n.d. <sup>f</sup>	n.d.	1.6 ± 0.2	n.d.	1.7
GMB <sup>+</sup> C CGCG	80 ± 27	28 ± 13	2130	n.d.	n.d.	0.89 ± 0.05	n.d.	0.92
GCGC CGMG	$K_{d1} \gg K_{d2}$		4400 ± 630	28 ± 4	7 ± 4	2.3 ± 1.3	1.4	0.94
B <sup>-</sup> CGC CGMG	$K_{d1} \gg K_{d2}$		890 ± 60	13.7 ± 0.3	3.6 ± 0.3	0.36 ± 0.01	0.73	0.14
B <sup>+</sup> CGC CGMG	$K_{d1} \gg K_{d2}$		1200 ± 190	17 ± 12	3.6 ± 0.8	0.87 ± 0.03	0.73	0.45
GCB <sup>-</sup> C CGMG	$K_{d1} \gg K_{d2}$		870 ± 120	18 ± 1	5.0 ± 0.6	0.39 ± 0.01	1.0	0.15
GCB <sup>+</sup> C CGMG	$K_{d1} \gg K_{d2}$		990 ± 80	17 ± 4	3.2 ± 0.6	0.36 ± 0.01	0.65	0.15

<sup>a</sup>The recognition site of Dnm13a-CD is marked in bold, while the cytosine to be methylated is underlined.

<sup>b</sup>Proportion of DNA converted at the end of the reaction in assays conducted at  $[E_2]_0 > [S]_0$ .

<sup>c</sup>The initial rate of methylation measured with 100 to 300 nM substrate and normalized to 300 nM substrate.

<sup>d</sup> Apparent catalytic constant obtained by dividing  $v_1$  by the concentration of the E<sub>4</sub>S complex in the corresponding assay. The E<sub>4</sub>S concentration was calculated using Scheme 1 with the  $K_{d1}$  and  $K_{d2}$  values specified in the table.

<sup>e</sup> Apparent catalytic constant obtained by dividing  $v_2$  by the concentration of the E4S complex in the corresponding assay.

<sup>f</sup> Not determined.